GLOBAL JOURNAL OF PURE AND APPLIED SCIENCES VOL 15, NO. 1, 2009: 117 - 124
 ISSN 1118-057

3D APPROACH OF SPECTRAL RESPONSE FOR A BIFACIAL SILICON SOLAR CELL UNDER A CONSTANT MAGNETIC FIELD

B. ZOUMA, A. S. MAIGA, M. DIENG, F. ZOUGMORE AND G. SISSOKO

(Received 25, May 2007; Revision Accepted 15, September 2008)

ABSTRACT

A three-dimensional study is made to improve the theoretical approach of spectral response of bifacial polycrystalline silicon solar cells. This study has allowed taking into account new parameters like grain size and grain boundaries recombination velocity, which reduce the cell efficiency. Losses in emitter region and external magnetic field are also being taken into account in order to perfect the description of measured spectral response. Then the new analytical expressions of carrier, photocurrent and short circuit densities are produced for front side and rear side illuminations. Homemade software based on the new analytical expressions of internal quantum efficiency is used to fit the experimental data.

PACS: *73.50.Pz*
KEYWORDS: 1-Spectral response; 2- Polycrystalline; 3- Solar cell; 4- Magnetic field.

1. INTRODUCTION

The spectral response (SR) data are useful to determine the quality of solar cells. From the SR, one can determine fundamental parameters of solar cells like: effective diffusion length (L_{eff}), effective lifetime (τ_{eff}), back surface recombination velocity (S_B), which are used in the characterization above. There exists a lot of techniques of characterization using SR data, but each of them uses its own theoretical approach of SR. We can cite the linear fit method (Warta, 1992.), (Werner, et al., 1993), (Basu and Singh, 1994, pp.317-329), (Spiegel, et al., 2000), (Tool et al., 2002); its application leads to L_{eff} directly and is suitable for solar cells where L_{eff} is much smaller than the base region thickness.

The theoretical approach of SR is better in producing accurate values of fundamental parameters. Thereby, the other parameters must be taken into account to describe SR especially for the polycrystalline silicon solar cells (Lu, et al., 2003) (Fedorov, et al., 2002, pp.49-55), which are mainly used in terrestrial applications. The grain size and the grain boundaries recombination velocity (S_g) (Lu, et al., 2003) (Ba, et al., 2003, pp.143–154) in polycrystalline silicon solar cells are important parameters which affect its efficiency.

During the SR measurement (Spiegel, et al., 2000), the influences of external conditions like the temperature and the magnetic field intensity are not outdone.

In this paper we make a new theoretical approach of the spectral response through a three dimensional study. In order to improve the SR, we are taking into account the contribution of emitter region, grain size, grain boundaries (GBs) recombination velocity, and an external magnetic field.

We also apply a new technique to determine the recombination parameters based on new expressions of spectral response by fitting experimental data.

This work is split into three parts: in the first part we have the theory that leads to the internal quantum efficiency, then in the second part we investigate the influence of magnetic field and GBs recombination and in the last part we present the new method and the results of its application.

2. MODELLING

2.1. Model and assumptions

In this study, we use a sample of polycrystalline bifacial silicon solar cell which is presented on figure1.

B. Zouma, Laboratoire de Matériaux et Environnement, Département de Physique,Unité de Formation et de Recherche en Sciences exactes et Appliquées, Université de Ouagadougou, Burkina Faso.
A. S. Maiga, Laboratoire des Semiconducteurs et d'Energie solaire, Département de Physique, Faculté des Sciences et Techniques, Université Cheikh Anta Diop, Dakar, Senegal.
M. Dieng, Laboratoire des Semiconducteurs et d'Energie solaire, Département de Physique, Faculté des Sciences et Techniques, Université Cheikh Anta Diop, Dakar, Senegal.
F. Zougmore, Laboratoire de Matériaux et Environnement, Département de Physique,Unité de Formation et de Recherche en Sciences exactes et Appliquées, Université de Ouagadougou, Burkina Faso.
G. Sissoko, Laboratoire des Semiconducteurs et d'Energie solaire, Département de Physique, Faculté des Sciences et Techniques, Université Cheikh Anta Diop, Dakar, Senegal.

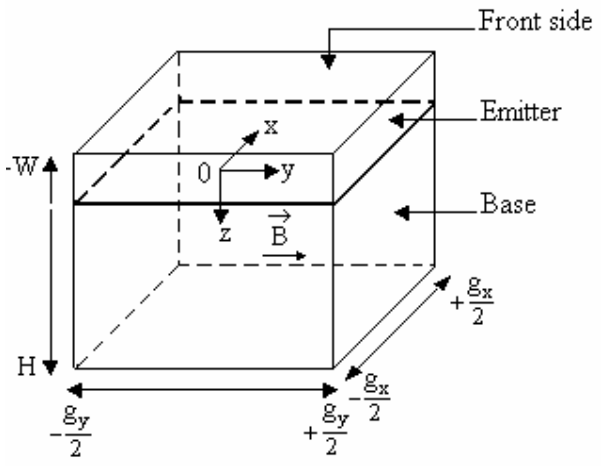

Figure 1: A grain in the columnar geometry

Assumptions:

1) The grains have square cross section (g_x= g_y=g) and their electrical properties are homogeneous. We can then use the Cartesian coordinates.
2) The grain boundaries (GBs) are perpendicular to junction and their recombination velocities are constant and independent of illumination so that the boundary conditions of continuity equations are linear.
3) The shadow effects of grids are neglected.
4) The grain boundaries velocity for the emitter region (S_{ge}) is the same for the base region (S_{gb}); S_{ge}= S_{gb}=S_g.
5) The magnetic field is constant and it is applied into the emitter and the base regions.

2.2. 3D equation of continuity

Applying the magnetic field as described above, the electron and the 3D hole equations of continuity are respectively given on eq.1 and eq.2

$$\frac{\partial^2 \delta_n}{\partial x^2} + \theta_n \frac{\partial^2 \delta_n}{\partial y^2} + \frac{\partial^2 \delta_n}{\partial z^2} - \frac{\delta_n}{L_n^{*2}} = -\frac{G}{D_n^{*2}} \quad (1)$$

$$\frac{\partial^2 \delta_p}{\partial x^2} + \theta_p \frac{\partial^2 \delta_p}{\partial y^2} + \frac{\partial^2 \delta_p}{\partial z^2} - \frac{\delta_p}{L_p^{*2}} = -\frac{G}{D_p^{*2}} \quad (2)$$

where δ is the carrier density, a function of spatial coordinates and the wavelength λ and can be written as $\delta(x,y,z,\lambda)$.

$$\theta = 1 + (\mu B)^2 \quad (3)$$

The diffusion coefficient

$$D^* = \frac{D}{\theta} \quad (4)$$

The diffusion length

$$L^{*2} = \frac{L^2}{\theta} \quad (5)$$

The indices n and p are respectively referring to the electron and to the hole.
The generation rate G on the right of equations 1 and 2 is a function of z and λ, it can be expressed as (Mohammad, 1987, pp.767-772), (Mandelis, 1989, pp. 5572-5583):

$$G(z,\lambda) = \alpha(\lambda)[1 - R(\lambda)]\phi_0(\lambda)[\beta e^{-\alpha(\lambda)[W + z]} + \gamma e^{-\alpha(\lambda)[H - z]}] \quad (6)$$

α and R are respectively the absorption and the reflexion coefficients. ϕ_0 is the incident electron beam.
The parameters β and γ determine illumination mode as described in table 1:

Table 1: parameters β and γ

Illumination mode	β	γ
Front side	1	0
Rear side	0	1

The resolution of these equations of continuity leads to the minority carrier densities. We have used the method of Ducas (Ducas, 1994, pp.71-88) with the boundary conditions:

- For the electrons in the base region

$$\left.\frac{\partial \delta_n(x,y,z,\lambda)}{\partial z}\right|_{z=0} = S_{Fn}\frac{\delta_n(x,y,0,\lambda)}{D_n^*} \tag{7}$$

$$\left.\frac{\partial \delta_n(x,y,z,\lambda)}{\partial z}\right|_{z=H} = -S_B\frac{\delta_n(x,y,H,\lambda)}{D_n^*} \tag{8}$$

Here, S_{Fn} is the recombination velocity at junction and S_B is the back surface recombination velocity.
- For the holes in the emitter region

$$\left.\frac{\partial \delta_p(x,y,z,\lambda)}{\partial z}\right|_{z=0} = -S_{Fp}\frac{\delta_p(x,y,0,\lambda)}{D_p^*} \tag{9}$$

$$\left.\frac{\partial \delta_p(x,y,z,\lambda)}{\partial z}\right|_{z=-W} = S_E\frac{\delta_p(x,y,-W,\lambda)}{D_p^*} \tag{10}$$

Where, S_{Fp} is the recombination velocity at junction and S_E the front surface recombination velocity.
The expressions of the minority carrier densities are:

$$\delta_n(x,y,z,\lambda) = \sum_{i=0}^{\infty}\sum_{j=0}^{\infty} Z_{ni,j}(z,\lambda)\cos(C_i x)\cos\left(\frac{C_j}{\sqrt{\theta_n}}y\right) \tag{11}$$

$$\delta_p(x,y,z,\lambda) = \sum_{i=0}^{\infty}\sum_{j=0}^{\infty} Z_{pi,j}(z,\lambda)\cos(C_i' x)\cos\left(\frac{C_j'}{\sqrt{\theta_p}}y\right) \tag{12}$$

Then, we can obtain the photocurrent densities from the densities above by the following relations:

$$J_n(\lambda) = \frac{qD_n^*}{g_x g_y}\int_{-\frac{g_x}{2}}^{+\frac{g_x}{2}}\int_{-\frac{g_y}{2}}^{+\frac{g_y}{2}}\left[\frac{\partial \delta_n(x,y,z,\lambda)}{\partial z}\right]_{z=0} dydx \tag{13}$$

$$J_p(\lambda) = -\frac{qD_n^*}{g_x g_y}\int_{-\frac{g_x}{2}}^{+\frac{g_x}{2}}\int_{-\frac{g_y}{2}}^{+\frac{g_y}{2}}\left[\frac{\partial \delta_p(x,y,z,\lambda)}{\partial z}\right]_{z=0} dydx \qquad (14)$$

2.3. The internal quantum efficiency

The internal quantum efficiency is deduced to the short circuit photocurrent density. This density is obtained from the above defined photocurrent density, the junction recombination velocity must be high (S_F>4.10^4 cm/s^1). When S_F increases, there are more and more carriers going through the junction.

Taking into account the contribution of the emitter region, the IQE can be expressed as:

$$IQE(\lambda) = \frac{Jsc_p(\lambda) + Jsc_n(\lambda)}{q\phi_0(\lambda)[1 - R(\lambda)]} \qquad (15)$$

Jsc_p is the hole short circuit photocurrent density and Jsc_n the electron short circuit photocurrent densities.

3. RESULTS OF SIMULATIONS

3.1. Emitter contribution on IQE

For pointing out the emitter contribution on the IQE, we have to compare the curves of IQE versus the wavelength for two theoretical expressions (Base only, Base + Emitter). These curves are plotted for a grain size g=0.01 cm with a magnetic field B = 5x10^{-5} T. Figure 1 concerns the front side illumination and Figure 2 the front side illumination.

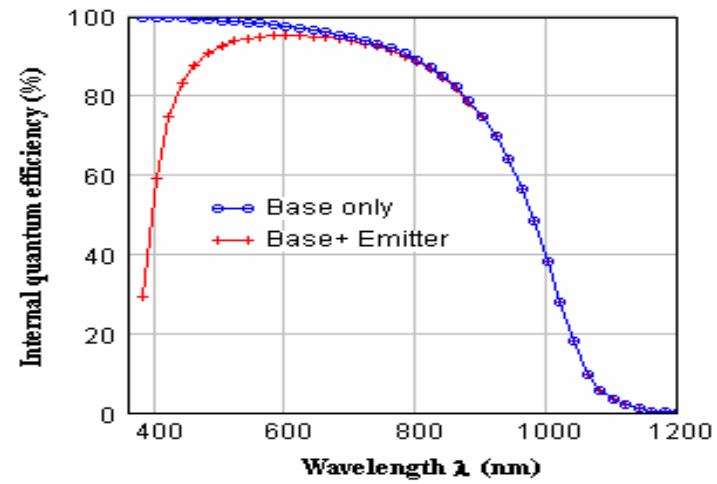

Figure 2: The curves of IQE versus λ for front side illumination with: H=299.9 µm, W=0.1 µm , Ln=100 µm, Lp=0.04 µm, g=0.01 cm , SB=2x10^2 cm/s, SE=3x10^3 cm/s, Sg=100 cm/s, B=5x10^{-5} T

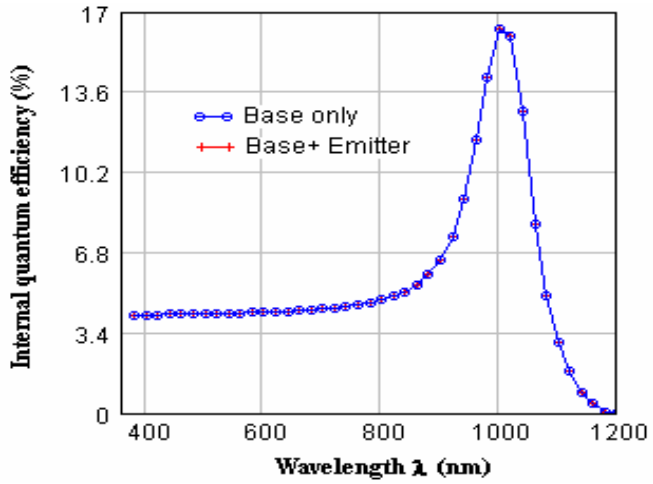

Figure 3: The curves of IQE versus λ for rear side illumination with: H=299.9 µm, W=0,1µm , Ln=100 µm, Lp=0.04 µm, g=0.01 cm, SB=3x10^3 cm/s, SE=2x10^2 cms^{-1}, Sg=100 cm/s, B=5x10^{-5} T.

We note that the contribution of the emitter region can be neglected when the solar rear side illuminated (figure 3) because the curves are confounded. But for the front side illumination (figure 2) the curves are different from 380 nm to 680 nm, and the contribution of emitter consists to reduce the IQE. In fact, for a front side illumination there are lots of generated holes in the emitter and most of them will be the traps of the electrons coming from the base region. The profile of IQE using the eq.15 is in a good agreement with the experimental spectral response (Meier, 1988)
The emitter region becomes the electron recombination areas when it is sufficiently illuminated. Taking into account the contribution allows one to improve the IQE analytical expression.

3.2. The magnetic field influence on the IQE

To determine the influence of the magnetic field on the IQE, we plot the 3D curves giving the variations for a grain size (g=0.01cm).
On figure 4 and figure 5, the 3D curves are presented respectively for the front side and rear side illuminations.

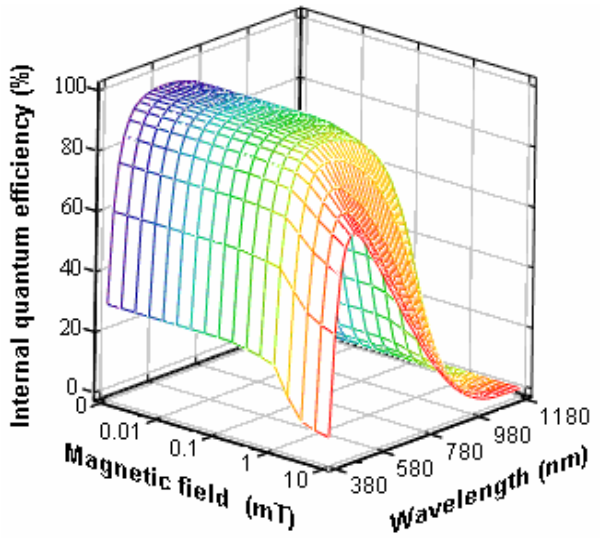

Figure 4: 3D curve of IQE for a front side illumination with: H=299.9 µm, W=0.1 µm Ln=100 µm, Lp=0.04 µm, g=0.01 cm , SB=2x10^2 cm/s, SE=3x10^3 cm/s, Sg=100 cm/s

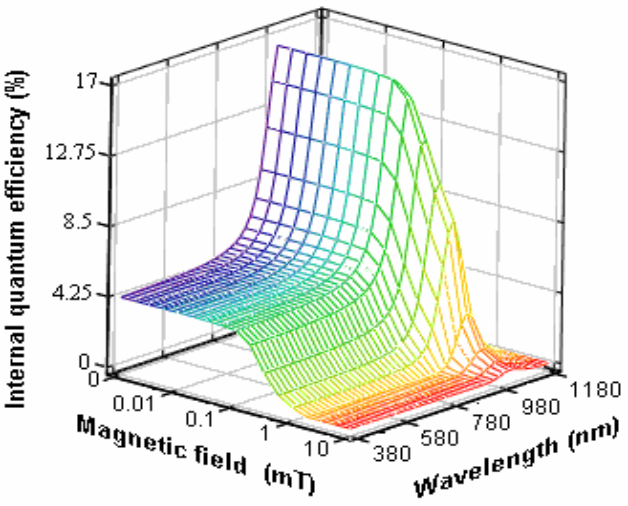

Figure 5: 3D curve of IQE for a rear side illumination with: H=299.9 µm, W=0.1µm Ln=100µm, Lp=0.04 µm, g=0.01 cm, SB=2x10^2 cm/s, SE=3x10^3 cm/s, Sg=100 cm/s

The IQE is heavy reduced for the magnetic field B>0.1 mT or (B>10^{-4} T), from this limit, the more B increases the more spectral response gets narrower (figure 4). The influence of magnetic fieldis pronounced for the rear side illumination; the magnetic field acts on the carriers of charge by reducing their diffusion coefficients. When a magnetic field is applied, the values of the diffusion coefficients change (see eq.4). When B increases, the diffusion coefficient decreases, the electrons and the holes are less mobile, and this

increases their recombination. For the rear side illumination (figure 5), there are more generated electrons near the back surface of the base region, they can not move to junction when a high magnetic field is applied and in addition this back surface is commonly a recombination zone.

In the figures above, for B<0.1 mT the variation of IQE is very weak, and then the influence the terrestrial magnetic which is around 0.05 mT, can be known. The terrestrial magnetic field can not affect seriously the efficiency polycrystalline silicon solar cells.

3.3. Influence of the grain boundaries recombination velocity

Now, the 3D curves are computed to point out the influence of S_g on the spectral response for a grain polycrystalline silicon solar cell (g=0.01 cm) under a constant magnetic field B=5x10^{-5} T. The GBs recombination velocity S_g is the same for the base and the emitter regions. The results are presented in figure 6 for the front side illumination and figure 7 for the rear side illumination.

For a given grain, the IQE decreases when the GBs recombination velocity S_g increases. When S_g>100 cm/s the IQE obtained for rear side illumination (figure 7) is heavily reduced; the good bifacial polycrystalline silicon solar cell must have S_g smaller than 100 cm/s.

The intensity of the GBs recombination in polycrystalline solar cell is also due to the grain size. This is because when the grains are very small, the solar cell contains several grains that increase the grain boundaries.

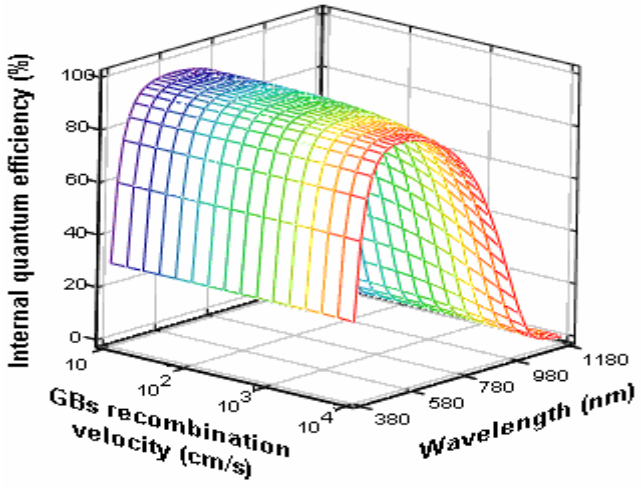

Figure 6: 3D curve of IQE for a front side illumination with: H=299.9 µm, W=0.1 µm, Ln=100 µm, Lp=0.04 µm, g=0.01 cm , SB=2x10^2 cm/s, SE=3x10^3 cm/s, and B=5x10^{-5} T

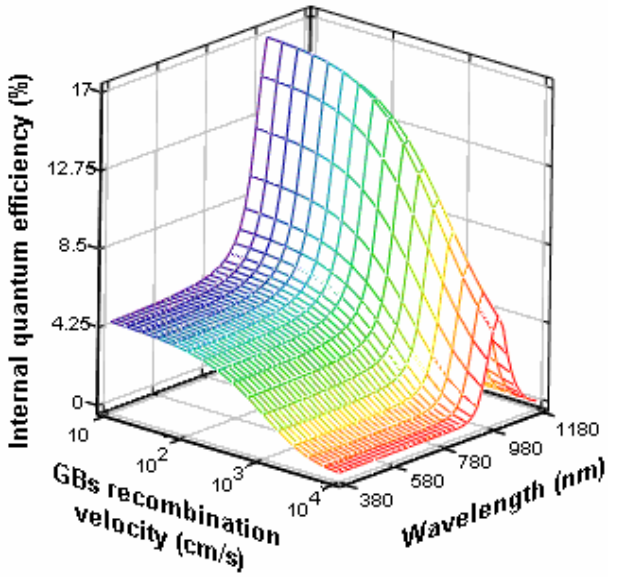

Figure 7: 3D curve of IQE for a rear side illumination with: H=299.9 µm, W=0.1 µm, L_n=100µm, L_p=0.04 µm, g=0.01 cm , S_B=2x10^2 cm/s, S_E=3x10^3 cm/s, B=5x10^{-5} T

4. METHOD OF CHARACTEIZATION

This method of characterization is developed from MathCAD software and is based on the fitting of experimental and theoretical data of the internal quantum efficiency. Here the theoretical data are generated by our expression of internal quantum efficiency. The IQE defined above is a function seven of parameters as: the effective electron diffusion length L_n, effective hole electron diffusion length L_p, the back surface

recombination velocity in the base region S_B, the front surface recombination velocity in the emitter region S_E, the grain size g, the GBs recombination velocity S_g and the external magnetic field intensity B.

Mathematically, the key parameter of this method is given by:

$$\sigma = \sqrt{\frac{1}{N - n_0} \sum_{i=n_0}^{N} (IQE - \eta)^2} \qquad (16)$$

IQE provides the theoretical data of efficiency and η provides the experimental data.

The quality of the fit depends on the value of □, smaller values producing better fits.

This method is very practical, and be used to determine the recombination parameters desired. It was applied for 2D modelling of spectral response; the determined recombination parameters are: the effective diffusion length, the back surface recombination velocity. We note that, grain size, GBs recombination velocity and the magnetic field have not been taking into account. The results are given in table2:

Table 2: determined recombination parameters

	Cell Q37C H=160 µm	Cell Q68C H=150 µm	Cell Q7C H=140 µm
L_n experimental	36 µm	89 µm	200 µm
Front side illumination	σ=0.0188	σ=0.043	σ=0.057
	L_n=41 µm	L_n=86 µm	L_n=190 µm
	S_B=3x10^3 cm/s	S_B=200 cm/s	S_B=200 cm/s
Rear side illumination	σ=0.016	σ=0.029	σ=0.072
	L_n=31 µm	L_n=95 µm	L_n=195 µm
	S_B=5x10^5 cm/s	S_B=4x10^4 cm/s	S_B=350 cm/s

The other characteristics of cells Q37C, Q68 and Q7C are given in (Meier et al., 1988).

The analysis of table 2 shows a good fit with the cells Q37C and Q68C. For these cells the diffusion length is smaller than the base thickness, and the difference between experimental and theoretical values is not so big for σ<0. 05.

When the diffusion length is bigger than the base thickness, σ>0.05 increases the difference between experimental and theoretical values.

The values of the velocity S_B is decreasing when the diffusion length becomes more and bigger than the base thickness. The rear side illumination leads to the large values of S_B compared to the front side illumination, and is in a good agreement with the literature.

Generally the results of applying the method are in a good agreement with the experimental data and with the literature.

The basis of this method is the analytical expression of the spectral response (or internal quantum efficiency) and getting the accurate values of the recombination parameters needs an improved analytical expression of the IQE. Then the 3D study made in this paper provides this improved expression of the IQE.

Using the new expression of IQE, this method can predict an average of grain size and return account of a great number of the recombination phenomenon in the polycrystalline silicon solar cells.

CONCLUSION

This work has allowed us to establish an improved analytical expression of the internal quantum efficiency which takes into account the losses in the emitter region, the grain size, the grain boundaries recombination velocity and the terrestrial magnetic field. The influences of these parameters on the spectral response have been investigated and well known.

A judicious exploitation of the IQE expression is made by a new method of characterization using homemade software. The basis of this method is the analytical expression of IQE; it has to fit the experimental and theoretical data the spectral response. The results of an applying the method using a 3D modelling IQE are in good agreement with the experimental values.

REFERENCES

Ba, B., Kane M. and Sarr, J., 2003, Solar Energy Materials & Solar Cells 80: 143–154

Basu, P. K. and Singh, S. N., 1994, Solar Energy Materials and Solar Cells 33: 317-329

Ducas, J., 1994, Solar energy Materials and Solar cells 32: 71-88

Fedorov, A. A., Kolesnikova, A. L. and Ovid'ko, I. A., 2002, Mater.Phys.Mech. 5: 49-55.

Lu, J., Rozgonyi, G., Kordas, L. and Ciszek, T., 2003. NCPV and Solar Program Review Meeting

Mandelis, A., 1989, J. Appl. Phys 66: 5572-5583.

Meier, D.L., Hwang, J.M. and Campbell, R., 1988, IEEE transactions on electron devices vol. ED-3N.

Mohammad, S.N., 1987, J.Appl.Phys.61(2): 767-772

Spiegel, M., Fischer, B., Keller, S., and Bucher, E., 2000, 28th IEEE PVSC, Alaska.

Tool, C.J.J., Manshanden, P., Burgers, A.R., and Weeber, A.W., 2002, 28th IEEE PVSC, New Orleans.

Warta, W., 1992, 11th EC-PVSC

Werner, J.H., Kolodiniski, S., Rau, U., Arch, j. K., and Bauser, E., 1993, Appl. Phys. Lett.62 (23).